3D Genome

Subjects: Biochemistry & Molecular Biology | Genetics & Heredity

Contributor: Tapan Mohanta

The genome is the most functional part of a cell, and genomic contents are organized in a compact three-dimensional (3D) structure. The genome contains millions of nucleotide bases organized in its proper frame. Rapid development in genome sequencing and advanced microscopy techniques have enabled us to understand the 3D spatial organization of the genome. Chromosome capture methods using a ligation approach and the visualization tool of a 3D genome browser have facilitated detailed exploration of the genome.

3D genome topologically associated domain cohesin lamin chromosome capture hi-C capture C DNase circular chromosome conformation capture chromosome conformation capture carbon copy

1. Introduction

The genome, comprising both coding and non-coding DNA sequences, describes the genetic makeup of an organism [1][2]. The term ‘genome’ was coined by Hans Winkler in 1920, and it is now commonly used among researchers. Since the completion of high-quality reference genome sequences, we have witnessed several new discoveries in the ensuing decades, including genomic elements, structural and functional features of the genome, and genome organization [3][4][5][6][7][8]. An enormous amount of hierarchical compaction is required to produce three-dimensional (3D) chromatin structures from one-dimensional (1D) linear DNA sequences inside the nucleus under physical constraints [9][10][11]. The nucleus of a human cell contains 46 densely packed chromosomes [12]. In contrast, octoploid (*Opuntia*) [13], hexaploid (Sequoia) [14], and tetraploid (*Coffea*) [15] genomes contain 88, 66, and 44 chromosomes, respectively. However, *Ophioglossum* contains 1260 (decaploid, 630 pairs) chromosomes per cell [16], and these chromosomes can directly and accurately segregate themselves to the next cell during mitosis. Additionally, a ciliated protozoon, *Oxytrichatri fallax*, contains 1260–1600 chromosomes, commonly called nanochromosomes (amphidiploid) [17]. It is possible to organize the numerous chromosomes present in a cell into functional compartments at different genomic scales by folding them into hierarchical domains.

A chromosome has a distinct status in the nucleus, known as a ‘chromosome territory’, which is further partitioned into chromosomal compartments (A/B), topologically associated domains (TADs), and chromatin loops, mediated by the CCCTC-binding factor (CTCF; **Figure 1**) [18][19][20]. Chromatin folding plays a vital role in gene regulation, and transcriptional control is associated with physical contacts between target genes and the respective enhancers [18][21]. However, the functional loop between the genes and the regulator domain is predominantly carried out within TADs (**Figure 2**) [18]. High-level DNA folding and packaging generate extensive contacts between different

genomic regions (**Figure 2**). These contacts can be in several forms, such as the folding architecture of proteins and chromatins and the proximity of DNA sequences to one another [22][23]. The packaging of chromosomes also brings them into contact with one another, as well as with the nuclear compartments, including the nucleolus and nuclear envelope (**Figure 2**) [24][25][26]. Cells progress through the cell cycle and undergo differentiation to form specialized cells [27]. The genetic information and function of a genome are not only associated with the epigenetic markers in the 1D linear DNA sequences, but also with their non-random spatial organization in the 3D nucleus. 3D chromatin organization is directly correlated with the functionality of the genome [28][29]. Chromosomes must undergo structural rearrangement leading to re-organization of contacts among the chromosomes (while maintaining the 3D structure of the genome) to influence transcription and function [30][31][32].

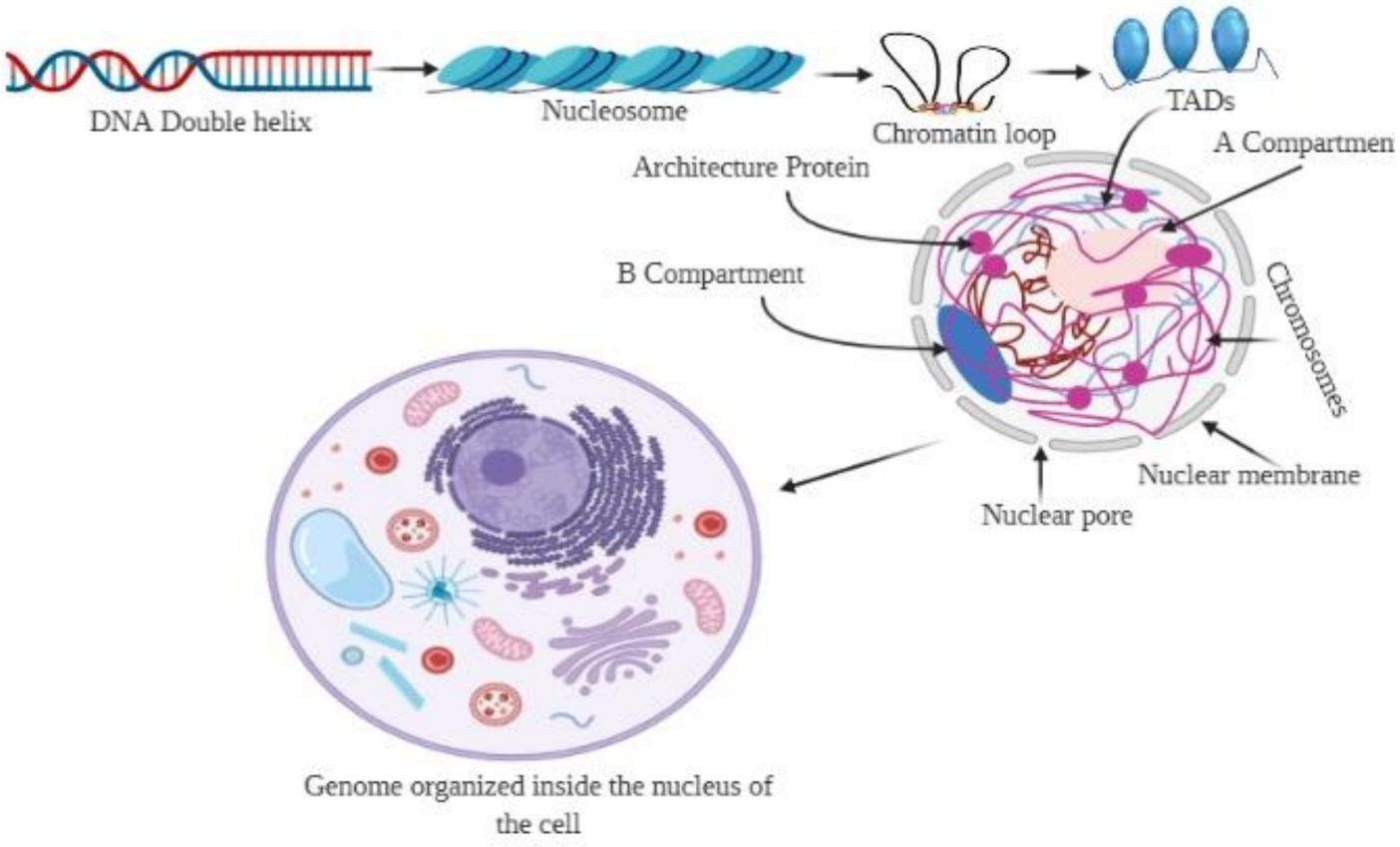

Figure 1. Organization of the 3D genome. The genomic DNA inside the nucleus possesses multiple levels of organizational structures. The primary structure, the linear DNA double helix, is packaged to form the secondary structural unit, nucleosome. The secondary structure brings approximately 7-fold compaction of genomic DNA. The 3D genome involves a higher-order organization in the 3D space of the nucleus, constituting topological features, including chromatin loops, A/B compartments, and chromosome territories. Chromatin loops are the basic building blocks for the 3D architecture of chromatins, while the topologically associated domains (TADs) are the basic structural and functional units of chromatins.

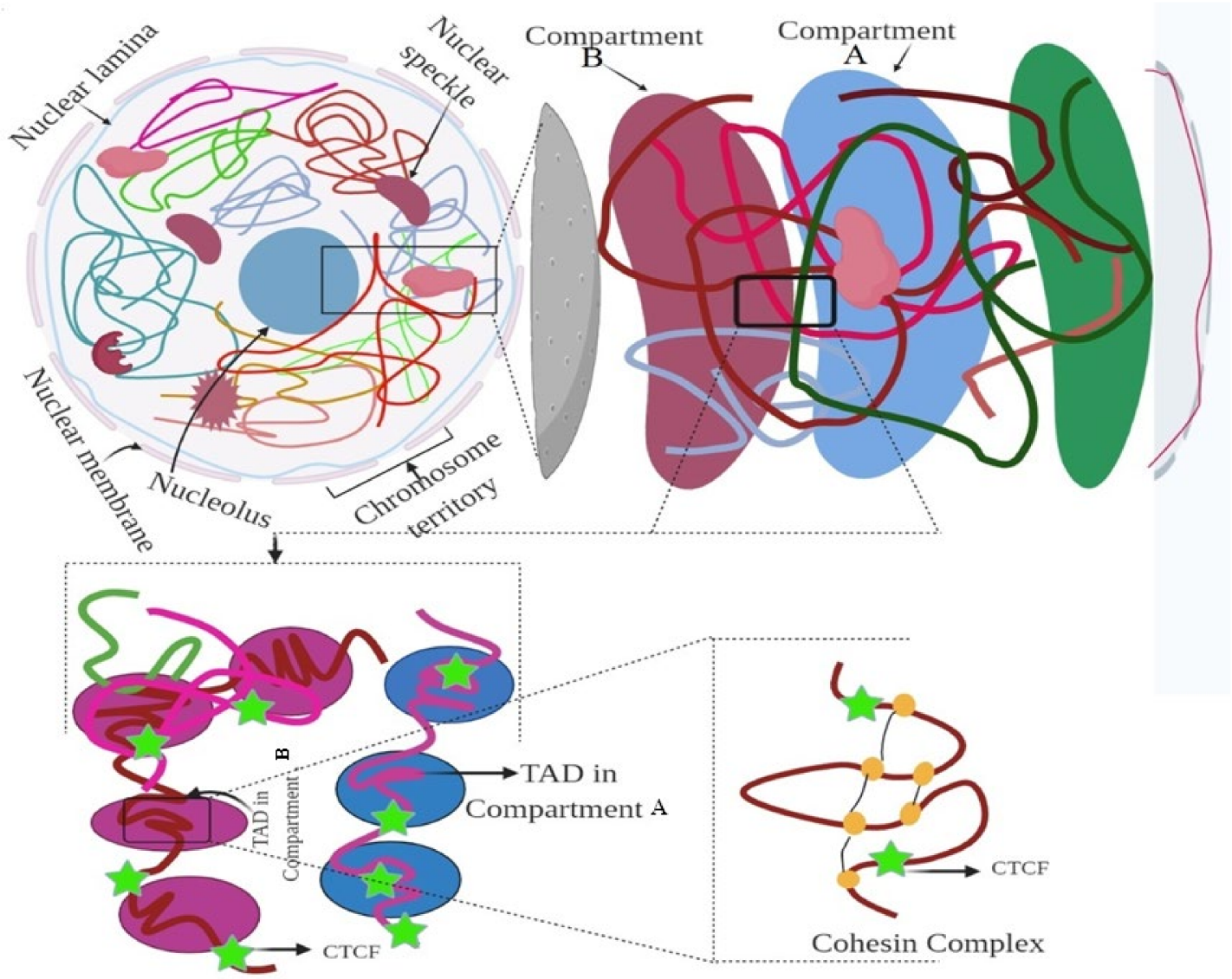

Figure 2. Hierarchical organization of the genome. Figure showing the nuclear compartment, CTCF, and TAD elements. The figure was prepared according to [9], with required modification.

Further, nuclear mechanobiology is one of the most important mechanical properties for nucleus adaptability, which maintains a proper 3D-shaped nucleus to facilitate the organization of a 3D genome [33]. The 3D structure of the nucleus is determined by the interplay of the cytoskeleton–nucleus links, integration and composition of the nuclear lamina, and degree of DNA packaging in the nucleus (**Figure 2**) [34][35][36].

Understanding how chromosomes are folded, packed, and positioned within the nucleus is of particular interest in deciphering the role of chromatin in gene regulation. Additionally, understanding the molecular distance between different genomic regions, or the molecular distance within the genomic regions and distinct nuclear compartments, can be of particular importance. To date, several methods have been developed to determine the architecture of a chromosome and its strengths and limitations. These include the chromosome conformation capture (3C) (**Figure 3**) [37][38][39] and high-throughput chromosome conformation capture (Hi-C) methods [29][40][41], which can be used to understand functional nuclear landmarks (splicing speckles and nuclear lamina) [18], chromosome territories [42],

and TADs [43], thus facilitating the understanding of how frequently two genomic loci interact (**Figure 2**). DNA-FISH is a revolutionary method that allows visualization of chromosomes and genes in the nucleus [44][45]. This method provides single-cell information and allows only a small number of genomic loci to be analysed at a time. A 3C-based approach based on proximity ligation of DNA ends up being associated with chromatin contact (**Table 1**, **Figure 3**) [46]. However, the Hi-C map provides genome-wide chromatin contacts of kilobases to a few megabases [47][48][49]. The recent development of orthogonal ligation-free approaches, including genome architecture mapping (GAM) [50][51][52], split pool recognition of interaction by tag extension (SPRITE) [53][54], and chromatin-interaction analysis through droplet-based and barcode-linked sequencing (ChIA-Drop) [55][56], have revealed novel aspects of chromatin organization. SPRITE, GAM, and ChIA-Drop chromatin contacts identify topological domains and help predict complex chromatin contacts associated with three or more DNA fragments and uncover specific contacts that span tens of megabases [18][50][52].

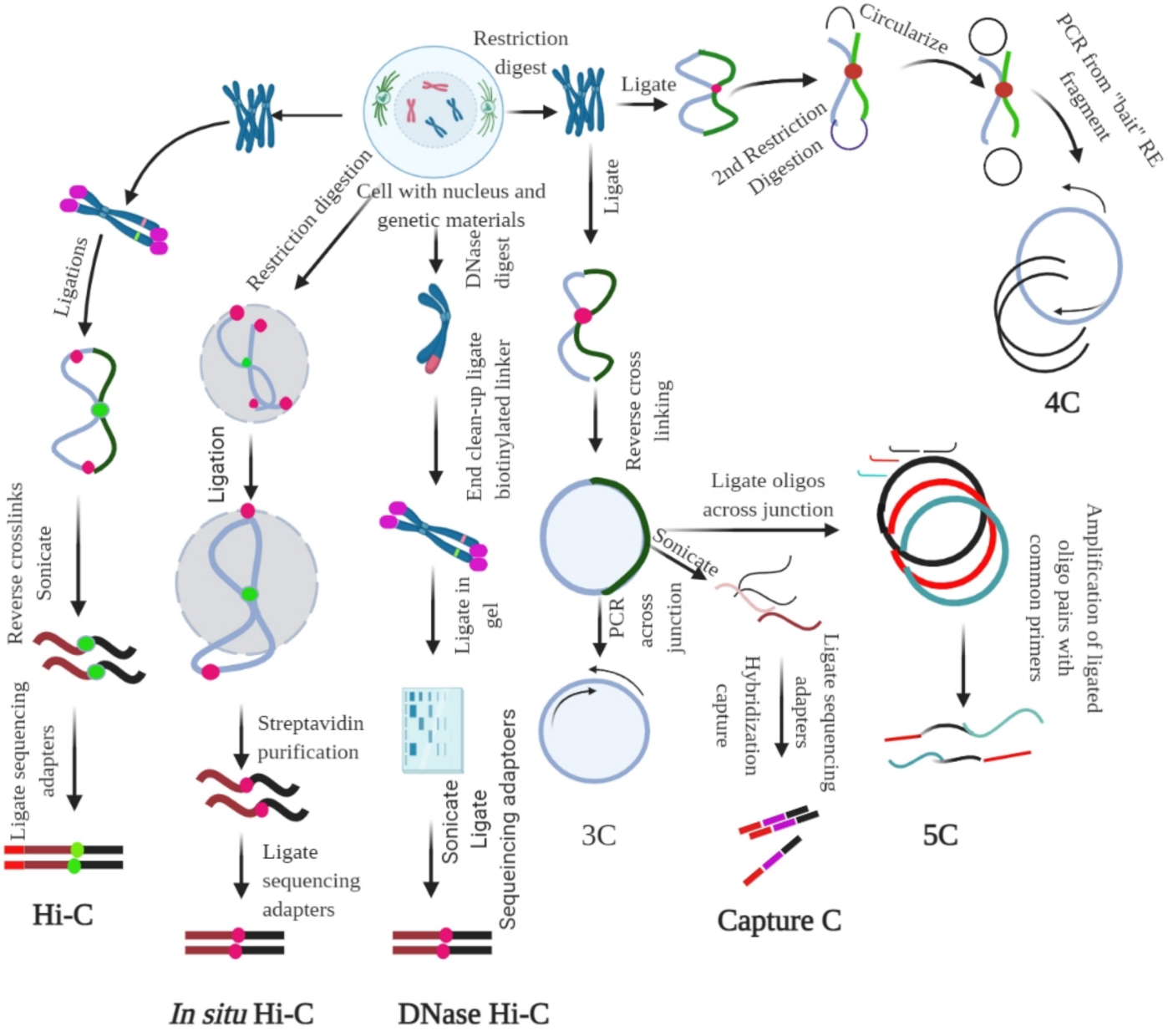

Figure 3. Chromosome conformation capture (3C) and its derivatives. It measures the contact frequencies of genomic loci by the proximity ligation of fragmented chromatin. All 3C procedures involve isolation of nuclei and DNA, followed by fixation of the chromatin. For Hi-C, ligation, followed by reverse cross-linking and addition of adaptors is required. For in situ Hi-C, streptavidin-based purification followed by the ligation of sequencing adaptors is required. For DNase Hi-C, the genetic materials are digested using DNase, followed by the ligation of biotinylated adaptor and adaptor-based sequencing. For 3C, restriction digestion is followed by ligation and reverse cross-linking and PCR across the junction. For capture C, reverse linking is followed by sonication, ligation of sequencing adaptors, and hybridization capture. In 5C, reverse cross-linking is followed by the ligation of oligos across the junction; the ligated oligo pairs are later amplified with a common primer. In 4C, restriction digestion and ligation are followed by the second step of restriction digestion, which circularize the genetic material; PCR is performed subsequently using the 'bait' RE fragment. The figure was prepared according to [18][57], with required modification.

Table 1. Table representing different chromosome conformation capture method and its application.

Method	Assay Type	Ligation Procedure	Characteristics
snHi-C	Whole genome to whole genome	Proximity ligation	3C variant used to map chromatin interaction
scHi-C	Whole genome to whole genome	Proximity ligation	Hi-C variant enable to map chromatin interaction at single cell
sciHi-C	Whole genome to whole genome	Proximity ligation	Enable mapping of chromatin interactions using combinatorial barcoding
3C	One locus to one locus	Proximity ligation	Founding method of 3C
4C	One locus to the genome	Proximity ligation	Method to detect chromatin interaction between a specific locus and rest of the genome

Method	Assay Type	Ligation Procedure	Characteristics
Enhanced ChIP-4C	One to one gene	Proximity ligation	A variant of 4C. It improves the sensitivity through replacement of inverse PCR with primer extension
Unique molecular identifier-4C	Detect chromosomal interaction between loci and conditions	Proximity ligation	Improved 4C variant for improved sensitivity and specificity. It uses molecular identifier to derive high-complexity quantitative chromatin contact profiles
5C		Proximity ligation	Method used to probe chromatin interaction of multiple loci
CAPTURE	One to one in the region of interest	Proximity ligation & biotinylation	Uses biotinylated dCas9-mediated locus specific chromatin interaction
Capture-3C	Whole genome	Proximity ligation	High throughput 4C that combines with 3C with DNA capture technology
Capture Hi-C	Whole genome	Proximity ligation	High throughput 4C that combines with Hi-C with DNA capture technology
Dilution Hi-C	Whole genome to whole genome	Biotinylated proximity ligation	Maps topological domains whose boarders are occupied by CTCF binding sites
RNA-TRAP	Locus to locus	Proximity biotinylation	Combination of RNA-FISH with ChIP to probe chromatin interaction

Method	Assay Type	Ligation Procedure	Characteristics
			associated with transcriptional active genes
Targeted DNAse Hi-C	Whole genome to whole genome	Proximity ligation	Combines DNase Hi-C with DNA capture technology
Associated chromosome trap	Long range allele specific/interchromosomal	Proximity ligation	Used to identify distant DNA region that interact with defined DNA target
ChIA-PET	Whole genome to whole genome mediated by protein of interest	Proximity ligation	Combines ChIP with proximity ligation to detect genome-wide chromatin interaction mediated by specific proteins
PLAC-Seq	Whole genome	Proximity ligation	Proximity ligation conducted in nuclei prior to chromatin shearing
HiChIP	Whole genome/Multi-scale	Proximity ligation	Combines 3C with ChIP to ascertain genome-wide chromatin interaction intervene by specific protein
Hi-C	Whole genome to whole genome	Proximity ligation	Used to map all chromatin interaction in a cell population
DNase Hi-C	Whole genome to whole genome	Proximity ligation	Is variant of Hi-C that uses DNase I to break the chromatin
In Situ Hi-C	Whole genome to whole genome	Proximity ligation	Is an in-situ version of Hi-C that uses chromatin digestion and

Method	Assay Type	Ligation Procedure	Characteristics
			proximity ligation of intact nuclei
Tethered chromosome conformation capture	Whole genome to whole genome	Proximity ligation	Similar to Hi-C, but ligation performed in solid substrate rather than solution
In Situ DNase Hi-C	Whole genome to whole genome	Proximity ligation	Hi-C variant that uses DNase to break the chromatin
Micro-C	Whole genome to whole genome	Proximity ligation	Is a variant of Hi-C that uses micrococcal nuclease to digest the chromatin
Bridge linker Hi-C	Whole genome	Proximity ligation	Used to capture structural and regulatory chromatin interaction by restriction enzymes
Chromosome walks	Whole genome	Proximity ligation	Links multiple genomic loci together into the proximity
Genome architecture mapping (GAM)	Whole genome	Co-localization	Enables identification of the interactions of enhancer and active genes across large genomic distance
Split pool recognition of interaction by tag extension (SPRITE)	Whole genome/interchromosomal [58][59][60][61][62][63][64][65] [62][66]	Co-association	Enables understanding of genome-wide detection of higher-order interactions within the nucleus

lied using
etermined
ıry nature
ridize the
eus [67][68]

permeabilized using detergents or organic solvents (for example, methanol). The DNA is denatured by heat and formaldehyde treatment and is visualized through a fluorescence microscope to ensure the fine binding of a probe with its target [69][70]. DNA FISH is used to visualize chromatin compaction and the positioning of genomic regions within the nucleus [71]. It can map the physical distance between two or more differentially labelled genomic

Method	Assay Type	Ligation Procedure [18][44][72]	Characteristics [73][74][75][76][77]
Multi-ChIA [78][79][80]	Locus to locus	Co-localization [18][82]	Mapping of multiplex chromatin interactions with single molecule precision. Allow mapping of chromatin interaction mediated by protein of interest [18][83]
Tethered conformation capture	Chromosome scale assembly [85][86]	Proximity biotinylation [18]	Allows mapping of inter and intrachromosomal contacts [84]

determine
ganization
t nuclear
are either
gments of
some [81].
use of the
cts within
ver, short-
chromatin
resolution
visualized
including

Oligopaints [87], can target 15-kb loci using conventional microscopy [80][87][88]. Oligopaints are libraries of synthesized oligonucleotides containing approximately 60–100 bp [89]. Subsequently, these oligonucleotides are amplified in a flexible manner using different primer pairs to generate FISH probes. Oligopaints can enable the study of chromatin folding in different epigenetic states at a resolution of tens of nanometers [90]. Oligopaint-based FISH, in combination with high-throughput imaging, can be useful for generating low-resolution contact maps, high-resolution contact maps (30 kb) for a stretch of 1.2–2.5 Mb, and maps for whole chromosomes [18][91].

2.2. Ligation-Based Detection of Contacts

3C is a one-on-one approach that can extract the chromatin interaction frequencies between two genomic loci via chromatin cross-linking and proximity ligation (**Figure 3**) [18][38]. Formaldehyde fixation is necessary for capturing protein-mediated and RNA-mediated contacts [38]. In the 3C method, the cells are cross-linked with formaldehyde, followed by fragmentation of chromatin using restriction digestion enzymes, such as HindIII or DpnII [92]. This is followed by proximity-based ligation of the adjacent DNA ends and determination of pairwise interactions using PCR sequencing. In the classical 3C method, a pair of interacting loci is interrogated using quantitative PCR, one at a time (**Figure 3**) [93]. This shows that 3C provides interactions between two loci and the required prior information of the target site (**Figure 3**).

Chromosome conformation capture-on-chip, commonly called 4C or circular chromosome conformation capture, is useful for interaction study of one region with the remaining part of the genome (one vs. all). The circular chromosome capture method, which is a part of the 3C technique, is used to address the existence of an epigenetically controlled network of chromosomal interactions. The 4C method is based on the principle of proximity ligation (**Table 1**), where the DNA–protein/protein–DNA generates a circular DNA molecule, using a high concentration of ligase and prolonged incubation for more than one week (**Figure 3**). Subsequently, reversal of the cross-linked primers proximal to the target sequence during ligation amplifies DNA with physical proximity, without prior knowledge of their identities. This procedure enables the amplification of sequences with a wide range of sizes in the cross-linked chromatin. 4C uses the same technology as 3C to obtain ligation products. The restriction

product ligates with the 3C template and is incubated overnight, with frequent cutting of the second restriction enzyme (DpnII/NlaIII) [86]. Subsequently, linear sequences are generated to conduct primer hybridization as a 4C template. These 4C templates are hybridized to an array according to the standard immunoprecipitation (ChIP) protocol. The nuclear organization of active and inactive chromatin domains can be uncovered by the 4C principle [86]. Additionally, long-range cis-interaction of the SOX9 promoter can also be analyzed using 4C analysis [94]. Additionally, all contacts can be mapped at a single locus using the 4C principle. Primers for a region (promoter/enhancer) can be used to amplify all ligation partners of the locus, followed by sequencing of the amplified product (depth of 1–5 million reads per library) [95]. This helps to analyze the genome-wide interaction partner of the region of interest at a resolution of a few kilobases. This procedure is well suited for detecting short-range regulatory interactions, long genomic distances, and whole chromosomes [86][96].

2.3. Non-Ligation-Based Detection

GAM is designed to analyze the 3D chromatin structure without the requirement of digestion and ligation [50]. It is based on the principle of linear genomic distance mapping to measure the 3D genome using ultrathin cryo-sectioning [97]. In GAM, cryo-sectioning of frozen fixed cells embedded in sucrose is performed in random orientation, followed by the generation of a single nuclear profile using laser microdissection. The nuclear profiles are subsequently subjected to sequencing, followed by sequence analysis. Once slices of the large collection of co-segregated possible pairs of loci in nuclear profiles are generated in random orientations, they are used to generate a proximity matrix of genomic regions. The GAM technique can map genome-wide chromatin contacts and is crucial for identifying topological domains. It can also detect highly complex chromatin contacts involving more than three DNA fragments and uncover specific contacts of approximately 10 Mb [18][50]. Further, GAM considers the spatial organization of chromatin architecture, including genome-wide contact frequencies, chromatin compaction, and the radial distribution of chromatin [50]. Beagrie et al. (2017) used 471 nuclear profiles of mouse embryonic stem cells using GAM procedures with a sequencing depth of 1.1 million reads per profile [50]. From this, they obtained 400,000 uniquely mapped reads per nuclear profile [50]. To understand the variation in detection, linkage disequilibrium was reported to be the best model to reduce bias. A comparison study with Hi-C and GAM revealed that they were highly correlated across the whole chromosome at a resolution of 1 Mb [50].

2.4. Cell Imaging of the Nuclear Structure

Chromosome folding is crucial for regulating proper gene expression and function, and it is a dynamic process that varies widely throughout the cell cycle [98][99]. TADs emerge as key players, leading to higher-order chromosome–chromosome folding, organization, and function through evolution. All these higher-order organizations are associated with tightly linked functional aspects, such as DNA replication and transcription. In relation to the genes associated with transcription, active genes are located more often toward the nuclear interior, even as the repressed genes are located toward the nuclear periphery (heterochromatic region) [100]. The chromosome-occupied distinct sub-nuclear territory is where the transcriptionally active loci are positioned at the surface. However, our ability to explore these genomic and chromatin dynamics has revolutionized technologies based on genome editing, which allows for simultaneous targeting of a particular locus in live cells. At present, genomic loci can be targeted in living cells using the clustered regularly interspaced short palindromic repeats (CRISPR)

system, which uses an endonuclease-deficient form of Cas9 (commonly called dead-Cas9 or dCas9), fused with a fluorescent protein [101]. The tagged dCas9 is applied to the genomic loci through its interaction with sequence-specific guided RNAs. However, for concurrent labelling of the two genomic regions, the guided RNAs should be modified to function as a scaffold that brings the fluorescent protein to the target loci. However, the CRISPR system is well suited for repetitive genomic sequences because it relies on a single type of guided RNA.

3. Hierarchy of the 3D Genome

The folding of DNA into chromosomes has become a focal point in the study of the 3D genome [102][103]. The spatial positioning of genes for important biological functions, such as DNA replication, transcription, DNA repair, and chromosome translocation, is of particular interest. The folding of nucleosomes and chromatin remains a highly debated topic [104]. Although the folding of DNA into nucleosomes is well known, it is unclear how the two interact with one another. The folding of large and complex chromosomes requires a structural hierarchy of chromatin loops to genes, and enhancers to chromosomal domains and nuclear compartments [105][106]. Chromosomal territories are the most significant components where DNA becomes organized [107]. The chromosomal loci located on the same chromosome interact more frequently, even when separated by 200 Mb, than any two loci located on different chromosomes [108][109]. Chromatin loops facilitate interactions between the two chromosome loci in the same chromosome [110]. The nuclear envelope plays a key role in 3D genome organization, confining the genomic DNA into the 3D space [111][112][113]. The inner nuclear membrane is lined with a meshwork of lamin proteins, thus forming the NL [114][115]. The NL interacts with the lamin-associated domain (LAD) [116][117], and almost half of the genomes of cells are composed of LADs (0.1–10 Mb; 553 kb). However, not all LADs interact with the NL. In different cells, a few chromosomes are not localized toward the nuclear periphery, suggesting cell-to-cell heterogeneity. LADs are considered heterochromatic regions and are characterized by the presence of low gene density and lack of transcription [118][119]. During cell division and differentiation, some LADs lose their association with the NL [120][121], while others associate with the nuclear periphery. This leads to the altered gene expression, where activated genes move toward the nuclear periphery and inactivated genes move toward the interior [122][123][124][125], found in LADs. The NL serves as an anchoring location for the genome and constitutes a place for the heterochromatic loci that are scattered throughout the genome, connecting with it in three dimensions [126][127][128]. When NL associates with heterochromatin, nuclear pore complexes (NPCs) are enriched for association with euchromatin and active genes [129][130]. Thus, the nuclear envelope should be considered an organizing surface. Similar to the LADs, there are also 0.1–10 Mb (749 kb)-sized nucleolus-associated domains, which are co-localized to nucleoli or the NL [131][132][133]. Chromosomes of similar sizes and gene densities interact more frequently than those with dissimilar sizes and gene densities, and they interact in the nuclear space [134][135]. Short and gene-dense chromosomes group together near the center of the nucleus, even as long and less gene-encoding chromosomes locate near the nuclear periphery [124][136].

4. 3D Genome and Gene Expression

Mechanical and biochemical signals perceived at the cell membrane activate transcription factors, which are subsequently directed to the target site to modulate cell- or tissue-specific gene expression [137][138][139]. When cells are placed on a substrate with different topographies, the nuclei change their shape, which leads to the activation of different gene expressions [140]. Cells placed on a different topography can exhibit distinct behaviors of proliferation, differentiation, and apoptosis [141][142]. Systemic turning of the contact area between the cell and extracellular matrix leads to altered gene expression of the matrix protein collagen [143]. Fibroblasts plated on polarized geometry express more matrix- or cytoskeleton-associated genes, whereas on isotropic surfaces, they express more cell–cell-junction and cell-cycle genes [140]. Nuclear architecture greatly shapes dynamic activities and expression of transcription factors, and with many genes, transcription occurs in bursts [144]. The transcription level is controlled by the burst frequency rather than the burst size [145]. Enhancer and promoter contacts, even in distant genomic loci, correlate with transcription, whereas the size of polymerase II correlates with the number of transcripts produced in a burst [146][147]. The temporal order of spatial clustering is a crucial aspect of gene co-regulation, and is necessary for activating various gene expression programs in different cell types [148][149][150]. During gene expression, genes are physically brought together. It may also involve the recruitment of transcription factors at different target sites and their subsequent clustering with other supporting transcription factor machinery [33]. It is highly possible that the integration and translation of biochemical cues into different gene expressions are enabled by different cellular and mechanical states [33]. The spatial organization of the genome has been optimized for cell-type-specific transcription, mediated by numerous mechanical and biochemical signals. Defects in mechano-signaling can lead to cell-to-cell contacts or an impaired extracellular matrix, which can lead to the disruption of the cytoskeleton–nucleus interaction, resulting in impaired nuclear morphology [151][152].

5. Data Structure of the 3D Genome

The close interaction between the 3D interphase DNA structure and gene expression has made chromatin folding a rapidly developing field of study. Several previous reports have been continuously challenged by the progress of research. For example, in the solenoid model, chromatin is folded into a 30-nm fibre, which is assembled into higher-order structures [153]. However, this report has not been substantiated when studied using electron microscopy tomography, which has shown highly distorted chromatin polymers [154]. We have discussed the role of TADs and the genomic contact and loop extrusion hypothesis based on CTCF and cohesin. It was previously thought that condensin compacts chromosomes by randomly bridging the DNA segment or supercoiling or passively pushing to sites of convergent transcription by RNA polymerase [155]. However, direct observation of loop extrusion in a single molecule has been found in condensin motor activity when quantum-dot-tagged yeast condensin was translocated along double-tethered DNA curtains [156]. The loop extrusion in the naked DNA was reported to be faster than that in DNA polymerase. While the loop extrusion of naked DNA translocation proceeded at a speed of 0.5–2 kb/s, those of DNA and RNA polymerases proceeded at approximately 1 kb/s and 1 kb/min, respectively [157][158]. The SMC complex uses ATP hydrolysis to perform the loop extrusion at a rate of 0.1–2 s^{-1} [155]. It has also been reported that cohesin- or condensin-binding factors possibly reduce the rate of chromatin loop extrusion. The major factors are the 11-nm nucleosome, RNA polymerase, protein complexes, and DNA structures [155]. However, the SMC complex can avoid these obstacles through nontopological binding, involving

intermittent interactions with Nipbl1 and Pds5 proteins that alter the extrusion dynamics, where Nipbl1 possibly acts as a ‘dynamic safety belt’ for the cohesin protein [155]. A recent study has explored these aspects and reported the presence of TAD-like clusters even after cohesin knockout [159][160]. These results suggest that large cooperation of the architectural regulatory proteins, as well as the interplay of supercoiling, molecular binding, phase separation, crowding effect, and loop extrusion events, is needed. There are also questions regarding the functional units of chromatin and their hierarchy of folding, and the inner functional units of working TADs at the single-cell level. To understand all these intricate events, researchers have applied mathematical rules (stochastic, self-returning event) and studied a folding algorithm that can replicate experimental observations [161]. The most common type of chromatin interaction in the genome is that of the promoter and enhancer for transcriptional regulation and heterogeneous packing, which disperses local DNA accessibility and allows transcription and nuclear transport. From a polymer physics point of view, there is an apparent conflict between these two chromatin properties. It has been reported that chromatin resembles a fractal globule, which is a self-similar polymer in a collapsed state [162] [163]. Although the fractal globule model observes high contact frequencies, it does not explain the spatial heterogeneity of chromatin packaging, which a 1D polymer cannot provide [161]. Therefore, researchers have provided a self-returning random walk (SRRW) mathematical model to address the contact-structure paradox [161]. It provides a non-branching topology of the 10-nm chromatin fiber and generates tree-like topological domains connected to an open chromatin backbone [161]. The SRRW model, presenting a new picture of genome organization, supports the hypothesis that local DNA density plays a critical role as a transcriptional regulator; the chromatin folds into a variety of minimally entangled hierarchical structures across the length from nanometers to micrometers without the necessity of a 30-nm fiber [161]. This model also explains the structure–function relationship of the interphase DNA with higher-order folding and a substantial reduction in dimension during genomic landscape exploration [161]. The model also predicts that the topological domains in single cells contain random-tree structures, where tree domains are regarded as nanoclusters and loops on a kilobase-to-megabase scale, serving as building blocks for large packaging domains. These tree domains are called ‘3D forests’ within the chromosome territory [161]. The size of a tree domain is positively correlated with the size of the genome, with considerable depression [161]. There is also a positive correlation between the tree domain size and packaging density, suggesting a size-dependent domain activity, where the nanodomain of the peak radius is approximately 70 nm [161]. Additionally, the model predicts a correlation between local DNA density and domain size, supporting the view that small domains are more active than large domains [161]. The first-order genome of a double helix DNA evolves to adopt a ‘virtual tree data structure’ for higher-order genome organization [161]. This tree-like topological domain is connected by an open functional backbone segment, which facilitates the proper organization of genomic contacts, package-based regulation of transcription, transport and accommodation of nuclear proteins, and transition between the interphase and mitosis [161].

A computational string and binder (SBS) model was proposed in polymer physics to understand the mechanism of chromosome compartmentalization, pattern formation, and chromatin folding [164]. According to the SBS model, chromatin folding can be driven thermodynamically by homotypic interactions between DNA sites that share compatible chromatin marks [164][165][166][167][168]. The chromatin filament acts as a self-avoiding walk string of beads, where specific beads function as binding sites for a cognate diffusing binder that can bridge them to allow

folding [164]. The different binding sites can selectively interact with their cognate binder, and these binding activities can be computationally investigated by molecular dynamics simulations using Langevin dynamics with classical interaction potential [164][168]. This model explains chromatin folding thermodynamically by homotypic interactions between DNA sites sharing cognate chromatin [166][167][168][169][170]. This interaction takes place via protein binding to multiple sites, inducing phase separation of chromatin sub-compartments [171]. The association between chromatin sites and the nuclear lamina and speckles can also be inferred using the SBS model, with the help of the bridging protein transcription factor YY1, RNA polymerase II, and Polycomb repressive complex 1 [164][172].

6. 3D Genome Browser

The role of an enhancer that resides in the proximity of its target genes and the role of TADs are well known. The volume of the chromatin interaction data increases regularly, and efficient visualization and navigation of these data are the major bottlenecks for their interpretation. These factors make it a daunting task for an individual laboratory to store and explore them properly. To overcome these problems, several visualization tools have been developed, with unique features and limitations. The Hi-C data browser is reportedly the first web-based query tool to visualize Hi-C data as heat maps [109]. However, it does not support zoom functionalization and can hold only a limited number of datasets. The WashU epigenome browser visualizes Hi-C and ChIA-PET data, which also enables access to thousands of epigenome datasets from ENCODE and the Roadmap epigenome project (**Figure 4**) [173] [174]. A Hi-C data matrix of files with large sizes up to hundreds of gigabytes tends to slow down the visualization process. Furthermore, it does not have the option to display inter-chromosomal interaction data as in a heat map. Hi-C data can also be explored using Juicebox [175] and Hi-Glass [176] at high speeds. However, none of these provides chromatin data, such as Capture Hi-C or ChIA-PET (**Table 1**, **Figure 4**). The Delta browser can display Hi-C data and a physical view of 3D genome modelling [177]. The 3D genome browser can help explore chromatin interaction data at the domain level and provide high-resolution promoter–enhancer interactions [178]. The 3D genome browser can facilitate zoom and traverse functions in real time, enabling queries using genomic loci, gene names, or SNPs (**Figure 4**) [178]. A user can also incorporate the UCSC genome browser with the WashU epigenome browser and query the chromatin interaction data with thousands of genetic, epigenetic, and phenotypic datasets, using the 3D genome browser [178]. Additionally, users can add or modify existing data or upload their genome or epigenome data, as well as view Hi-C data by converting the contract matrix into an indexed binary file called the ‘binary upper triangular matrix’ (BUTLR file). Users need to host a BUTLR file on an HTTP server and provide the URL to the 3D genome browser to obtain the full advantage of all the features of the 3D genome browser without the need to upload Hi-C data [178].

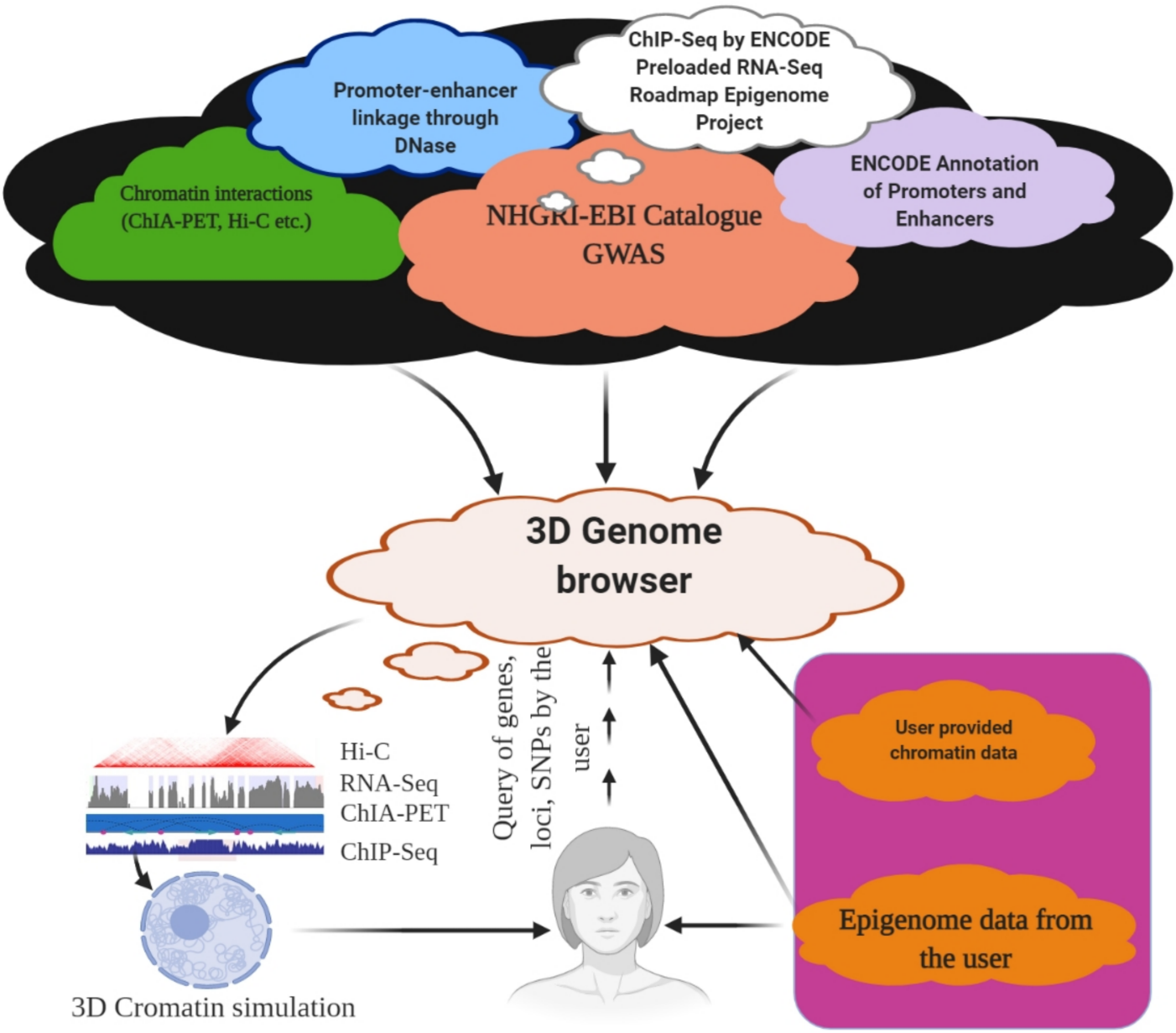

Figure 4. 3D Genome browser. Using a 3D genome browser, it is possible to join multiple users worldwide to explore and understand chromatin interaction data, including ChIA-PET, PLAC-Seq, Hi-C, and capture Hi-C.

References

1. Venter, J.C.; Adams, M.D.; Myers, E.W.; Li, P.W.; Mural, R.J.; Sutton, G.G.; Smith, H.O.; Yandell, M.; Evans, C.A.; Holt, R.A.; et al. The Sequence of the Human Genome. Science 2001, 291, 1304–1351.
2. Clamp, M.; Fry, B.; Kamal, M.; Xie, X.; Cuff, J.; Lin, M.F.; Kellis, M.; Lindblad-Toh, K.; Lander, E.S. Distinguishing protein-coding and noncoding genes in the human genome. Proc. Natl. Acad. Sci. USA 2007, 104, 19428–19433.

3. Church, D.M.; Schneider, V.A.; Graves, T.; Auger, K.; Cunningham, F.; Bouk, N.; Chen, H.-C.; Agarwala, R.; McLaren, W.M.; Ritchie, G.R.S.; et al. Modernizing Reference Genome Assemblies. PLoS Biol. 2011, 9, e1001091.
4. Tian, Y.; Zeng, Y.; Zhang, J.; Yang, C.; Yan, L.; Wang, X.; Shi, C.; Xie, J.; Dai, T.; Peng, L.; et al. High quality reference genome of drumstick tree (Moringa oleifera Lam.), a potential perennial crop. Sci. China Life Sci. 2015, 58, 627–638.
5. Li, Y.-C.; Korol, A.B.; Fahima, T.; Beiles, A.; Nevo, E. Microsatellites: Genomic distribution, putative functions and mutational mechanisms: A review. Mol. Ecol. 2002, 11, 2453–2465.
6. Razin, S.V.; Farrell, C.M.; Recillas-Targa, F.B.T.-I.R. Genomic Domains and Regulatory Elements Operating at the Domain Level. Int. Rev. Cytol. 2003, 226, 63–125.
7. Bernardi, G. THE HUMAN GENOME: Organization and Evolutionary History. Annu. Rev. Genet. 1995, 29, 445–476.
8. Parada, L.A.; Sotiriou, S.; Misteli, T. Spatial genome organization. Exp. Cell Res. 2004, 296, 64–70.
9. Zheng, H.; Xie, W. The role of 3D genome organization in development and cell differentiation. Nat. Rev. Mol. Cell Biol. 2019, 20, 535–550.
10. Rowley, M.J.; Nichols, M.H.; Lyu, X.; Ando-Kuri, M.; Rivera, I.S.M.; Hermetz, K.; Wang, P.; Ruan, Y.; Corces, V.G. Evolutionarily Conserved Principles Predict 3D Chromatin Organization. Mol. Cell 2017, 67, 837–852.e7.
11. Wang, S.; Xu, J.; Zeng, J. Inferential modeling of 3D chromatin structure. Nucleic Acids Res. 2015, 43, e54.
12. Tjio, J.H.; Levan, A. The Chromosome Number of Man. In Problems of Birth Defects: From Hippocrates to Thalidomide and After; Persaud, T.V.N., Ed.; Springer: Dordrecht, The Netherlands, 1977; pp. 112–118. ISBN 978-94-011-6621-8.
13. Felker, P.; Paterson, A.; Jenderek, M.M. Forage potential of Opuntia clones maintained by the USDA, National Plant Germplasm System (NPGS) collection. Crop Sci. 2006, 46, 2161–2168.
14. Breidenbach, N.; Sharov, V.V.; Gailing, O.; Krutovsky, K.V. De novo transcriptome assembly of cold stressed clones of the hexaploid Sequoia sempervirens (D. Don) Endl. Sci. Data 2020, 7, 239.
15. Cenci, A.; Combes, M.-C.; Lashermes, P. Genome evolution in diploid and tetraploid Coffea species as revealed by comparative analysis of orthologous genome segments. Plant Mol. Biol. 2012, 78, 135–145.
16. Sinha, B.M.B.; Srivastava, D.P.; Jha, J. Occurrence of Various Cytotypes of Ophioglossum reticulatum L. in a Population from N. E. India. Caryologia 1979, 32, 135–146.

17. Swart, E.C.; Bracht, J.R.; Magrini, V.; Minx, P.; Chen, X.; Zhou, Y.; Khurana, J.S.; Goldman, A.D.; Nowacki, M.; Schotanus, K.; et al. The Oxytricha trifallax Macronuclear Genome: A Complex Eukaryotic Genome with 16,000 Tiny Chromosomes. PLoS Biol. 2013, 11, e1001473.
18. Kempfer, R.; Pombo, A. Methods for mapping 3D chromosome architecture. Nat. Rev. Genet. 2020, 21, 207–226.
19. Szabo, Q.; Bantignies, F.; Cavalli, G. Principles of genome folding into topologically associating domains. Sci. Adv. 2019, 5, eaaw1668.
20. Kim, S.; Yu, N.-K.; Kaang, B.-K. CTCF as a multifunctional protein in genome regulation and gene expression. Exp. Mol. Med. 2015, 47, e166.
21. Krijger, P.H.L.; de Laat, W. Regulation of disease-associated gene expression in the 3D genome. Nat. Rev. Mol. Cell Biol. 2016, 17, 771–782.
22. Cubeñas-Potts, C.; Corces, V.G. Architectural proteins, transcription, and the three-dimensional organization of the genome. FEBS Lett. 2015, 589, 2923–2930.
23. Todolli, S.; Perez, P.J.; Clauvelin, N.; Olson, W.K. Contributions of Sequence to the Higher-Order Structures of DNA. Biophys. J. 2017, 112, 416–426.
24. Zhao, Y.; Zhan, Q. Electric oscillation and coupling of chromatin regulate chromosome packaging and transcription in eukaryotic cells. Theor. Biol. Med. Model. 2012, 9, 27.
25. Gavrilov, A.A.; Shevelyov, Y.Y.; Ulianov, S.V.; Khrameeva, E.E.; Kos, P.; Chertovich, A.; Razin, S. V Unraveling the mechanisms of chromatin fibril packaging. Nucleus 2016, 7, 319–324.
26. Luzhin, A.V.; Flyamer, I.M.; Khrameeva, E.E.; Ulianov, S.V.; Razin, S.V.; Gavrilov, A.A. Quantitative differences in TAD border strength underly the TAD hierarchy in Drosophila chromosomes. J. Cell. Biochem. 2019, 120, 4494–4503.
27. Jakoby, M.; Schnittger, A. Cell cycle and differentiation. Curr. Opin. Plant Biol. 2004, 7, 661–669.
28. Bonev, B.; Cavalli, G. Organization and function of the 3D genome. Nat. Rev. Genet. 2016, 17, 661–678.
29. Kong, S.; Zhang, Y. Deciphering Hi-C: From 3D genome to function. Cell Biol. Toxicol. 2019, 35, 15–32.
30. Eichler, E.E.; Sankoff, D. Structural Dynamics of Eukaryotic Chromosome Evolution. Science 2003, 301, 793–797.
31. Chen, Z.J. Genetic and Epigenetic Mechanisms for Gene Expression and Phenotypic Variation in Plant Polyploids. Annu. Rev. Plant Biol. 2007, 58, 377–406.
32. Tang, Z.; Luo, O.J.; Li, X.; Zheng, M.; Zhu, J.J.; Szalaj, P.; Trzaskoma, P.; Magalska, A.; Wlodarczyk, J.; Ruszczycki, B.; et al. CTCF-Mediated Human 3D Genome Architecture Reveals

Chromatin Topology for Transcription. Cell 2015, 163, 1611–1627.

33. Uhler, C.; Shivashankar, G. V Regulation of genome organization and gene expression by nuclear mechanotransduction. Nat. Rev. Mol. Cell Biol. 2017, 18, 717–727.
34. Starr, D.A.; Fridolfsson, H.N. Interactions between nuclei and the cytoskeleton are mediated by SUN-KASH nuclear-envelope bridges. Annu. Rev. Cell Dev. Biol. 2010, 26, 421–444.
35. Li, Q.; Kumar, A.; Makhija, E.; Shivashankar, G. V The regulation of dynamic mechanical coupling between actin cytoskeleton and nucleus by matrix geometry. Biomaterials 2014, 35, 961–969.
36. Maniotis, A.J.; Chen, C.S.; Ingber, D.E. Demonstration of mechanical connections between integrins, cytoskeletal filaments, and nucleoplasm that stabilize nuclear structure. Proc. Natl. Acad. Sci. USA 1997, 94, 849–854.
37. Hakim, O.; Misteli, T. SnapShot: Chromosome confirmation capture. Cell 2012, 148, 1068.e1–1068.e2.
38. Dekker, J.; Rippe, K.; Dekker, M.; Kleckner, N. Capturing Chromosome Conformation. Science 2002, 295, 1306–1311.
39. De Wit, E.; de Laat, W. A decade of 3C technologies: Insights into nuclear organization. Genes Dev. 2012, 26, 11–24.
40. Van Berkum, N.L.; Lieberman-Aiden, E.; Williams, L.; Imakaev, M.; Gnirke, A.; Mirny, L.A.; Dekker, J.; Lander, E.S. Hi-C: A method to study the three-dimensional architecture of genomes. J. Vis. Exp. 2010, 1869.
41. Belton, J.-M.; McCord, R.P.; Gibcus, J.H.; Naumova, N.; Zhan, Y.; Dekker, J. Hi–C: A comprehensive technique to capture the conformation of genomes. Methods 2012, 58, 268–276.
42. Nagano, T.; Lubling, Y.; Stevens, T.J.; Schoenfelder, S.; Yaffe, E.; Dean, W.; Laue, E.D.; Tanay, A.; Fraser, P. Single-cell Hi-C reveals cell-to-cell variability in chromosome structure. Nature 2013, 502, 59–64.
43. Melo, U.S.; Schöpflin, R.; Acuna-Hidalgo, R.; Mensah, M.A.; Fischer-Zirnsak, B.; Holtgrewe, M.; Klever, M.-K.; Türkmen, S.; Heinrich, V.; Pluym, I.D.; et al. Hi-C Identifies Complex Genomic Rearrangements and TAD-Shuffling in Developmental Diseases. Am. J. Hum. Genet. 2020, 106, 872–884.
44. Giorgetti, L.; Heard, E. Closing the loop: 3C versus DNA FISH. Genome Biol. 2016, 17, 215.
45. Bolland, D.J.; King, M.R.; Reik, W.; Corcoran, A.E.; Krueger, C. Robust 3D DNA FISH using directly labeled probes. J. Vis. Exp. 2013, 50587.
46. Übelmesser, N.; Papantonis, A. Technologies to study spatial genome organization: Beyond 3C. Brief. Funct. Genomics 2019, 18, 395–401.

47. Hansen, A.S.; Cattoglio, C.; Darzacq, X.; Tjian, R. Recent evidence that TADs and chromatin loops are dynamic structures. Nucleus 2018, 9, 20–32.
48. Kaul, A.; Bhattacharyya, S.; Ay, F. Identifying statistically significant chromatin contacts from Hi-C data with FitHiC2. Nat. Protoc. 2020, 15, 991–1012.
49. Eijsbouts, C.Q.; Burren, O.S.; Newcombe, P.J.; Wallace, C. Fine mapping chromatin contacts in capture Hi-C data. BMC Genomics 2019, 20, 77.
50. Beagrie, R.A.; Scialdone, A.; Schueler, M.; Kraemer, D.C.A.; Chotalia, M.; Xie, S.Q.; Barbieri, M.; de Santiago, I.; Lavitas, L.-M.; Branco, M.R.; et al. Complex multi-enhancer contacts captured by genome architecture mapping. Nature 2017, 543, 519–524.
51. Liu, T.; Wang, Z. normGAM: An R package to remove systematic biases in genome architecture mapping data. BMC Genomics 2019, 20, 1006.
52. Le Treut, G.; Képès, F.; Orland, H. A Polymer Model for the Quantitative Reconstruction of Chromosome Architecture from HiC and GAM Data. Biophys. J. 2018, 115, 2286–2294.
53. Rusk, N. SPRITE maps the 3D genome. Nat. Methods 2018, 15, 572.
54. Quinodoz, S.A.; Ollikainen, N.; Tabak, B.; Palla, A.; Schmidt, J.M.; Detmar, E.; Lai, M.M.; Shishkin, A.A.; Bhat, P.; Takei, Y.; et al. Higher-Order Inter-chromosomal Hubs Shape 3D Genome Organization in the Nucleus. Cell 2018, 174, 744–757.e24.
55. Koch, L. Getting the drop on chromatin interaction. Nat. Rev. Genet. 2019, 20, 192–193.
56. Zheng, M.; Tian, S.Z.; Capurso, D.; Kim, M.; Maurya, R.; Lee, B.; Piecuch, E.; Gong, L.; Zhu, J.J.; Li, Z.; et al. Multiplex chromatin interactions with single-molecule precision. Nature 2019, 566, 558–562.
57. Risca, V.I.; Greenleaf, W.J. Unraveling the 3D genome: Genomics tools for multiscale exploration. Trends Genet. 2015, 31, 357–372.
58. Schwarzacher, T.; Anamthawat-Jónsson, K.; Harrison, G.E.; Islam, A.K.M.R.; Jia, J.Z.; King, I.P.; Leitch, A.R.; Miller, T.E.; Reader, S.M.; Rogers, W.J.; et al. Genomic in situ hybridization to identify alien chromosomes and chromosome segments in wheat. Theor. Appl. Genet. 1992, 84, 778–786.
59. Fukui, K.; Ohmido, N.; Khush, G.S. Variability in rDNA loci in the genus Oryza detected through fluorescence in situ hybridization. Theor. Appl. Genet. 1994, 87, 893–899.
60. Trouvelot, S.; van Tuinen, D.; Hijri, M.; Gianinazzi-Pearson, V. Visualization of ribosomal DNA loci in spore interphasic nuclei of glomalean fungi by fluorescence in situ hybridization. Mycorrhiza 1999, 8, 203–206.

61. Shakoori, A.R. Fluorescence In Situ Hybridization (FISH) and Its Applications. Chromosom. Struct. Aberrations 2017, 343–367.
62. Cui, C.; Shu, W.; Li, P. Fluorescence In situ Hybridization: Cell-Based Genetic Diagnostic and Research Applications. Front. Cell Dev. Biol. 2016, 4, 89.
63. Bishop, R. Applications of fluorescence in situ hybridization (FISH) in detecting genetic aberrations of medical significance. Biosci. Horizons Int. J. Student Res. 2010, 3, 85–95.
64. Safak, Y.L.; Daniel, R.N. Mechanistic Approach to the Problem of Hybridization Efficiency in Fluorescent In Situ Hybridization. Appl. Environ. Microbiol. 2004, 70, 7126–7139.
65. Solanki, S.; Ameen, G.; Zhao, J.; Flaten, J.; Borowicz, P.; Brueggeman, R.S. Visualization of spatial gene expression in plants by modified RNAscope fluorescent in situ hybridization. Plant Methods 2020, 16, 1–9.
66. Diot, C.; Chin, A.; Lécuyer, E. Optimized FISH methods for visualizing RNA localization properties in Drosophila and human tissues and cultured cells. Methods 2017, 126, 156–165.
67. Johnson, M.D., III; Fresco, J.R. Third-strand in situ hybridization (TISH) to non-denatured metaphase spreads and interphase nuclei. Chromosoma 1999, 108, 181–189.
68. Egozcue, J.; Blanco, J.; Vidal, F. Chromosome studies in human sperm nuclei using fluorescence in-situ hybridization (FISH). Hum. Reprod. Update 1997, 3, 441–452.
69. Alamri, A.; Nam, J.Y.; Blancato, J.K. Fluorescence In Situ Hybridization of Cells, Chromosomes, and Formalin-Fixed Paraffin-Embedded Tissues. In Molecular Profiling: Methods and Protocols; Espina, V., Ed.; Springer: New York, NY, USA, 2017; pp. 265–279. ISBN 978-1-4939-6990-6.
70. Solovei, I.; Cavallo, A.; Schermelleh, L.; Jaunin, F.; Scasselati, C.; Cmarko, D.; Cremer, C.; Fakan, S.; Cremer, T. Spatial Preservation of Nuclear Chromatin Architecture during Three-Dimensional Fluorescence in Situ Hybridization (3D-FISH). Exp. Cell Res. 2002, 276, 10–23.
71. Fields, B.D.; Nguyen, S.C.; Nir, G.; Kennedy, S. A multiplexed DNA FISH strategy for assessing genome architecture in Caenorhabditis elegans. eLife 2019, 8, e42823.
72. Karafiátová, M.; Bartoš, J.; Kopecký, D.; Ma, L.; Sato, K.; Houben, A.; Stein, N.; Doležel, J. Mapping nonrecombining regions in barley using multicolor FISH. Chromosom. Res. 2013, 21, 739–751.
73. Moore, L.E.; Titenko-Holland, N.; Quintana, P.J.E.; Smith, M.T. Novel biomarkers of genetic damage in humans: Use of fluorescence in situ hybridization to detect aneuploidy and micronuclei in exfoliated cells. J. Toxicol. Environ. Health 1993, 40, 349–357.
74. Madon, P.F.; Athalye, A.S.; Sanghavi, K.; Parikh, F.R. Microdeletion Syndromes Detected by FISH–73 Positive from 374 Cases. Int. J. Hum. Genet. 2010, 10, 15–20.

75. ALmughamsi, M.M.; Kumosani, T.A.; ALhamzi, E.A.; Al-Qahtani, M. The use of fluorescence in situhybridization techniques in the detection of microdeletion syndromes. BMC Genomics 2014, 15, P60.

76. Masny, P.S.; Chan, O.Y.A.; de Greef, J.C.; Bengtsson, U.; Ehrlich, M.; Tawil, R.; Lock, L.F.; Hewitt, J.E.; Stocksdale, J.; Martin, J.H.; et al. Analysis of allele-specific RNA transcription in FSHD by RNA-DNA FISH in single myonuclei. Eur. J. Hum. Genet. 2010, 18, 448–456.

77. Rosin, L.F.; Gil, J., Jr.; Drinnenberg, I.A.; Lei, E.P. Oligopaint DNA FISH reveals telomere-based meiotic pairing dynamics in the silkworm, Bombyx mori. PLoS Genet. 2021, 17, e1009700.

78. Beliveau, B.J.; Kishi, J.Y.; Nir, G.; Sasaki, H.M.; Saka, S.K.; Nguyen, S.C.; Wu, C.; Yin, P. OligoMiner provides a rapid, flexible environment for the design of genome-scale oligonucleotide in situ hybridization probes. Proc. Natl. Acad. Sci. USA 2018, 115, E2183–E2192.

79. Torres-Ruiz, R.; Grazioso, T.P.; Brandt, M.; Martinez-Lage, M.; Rodriguez-Perales, S.; Djouder, N. Detection of chromosome instability by interphase FISH in mouse and human tissues. STAR Protoc. 2021, 2, 100631.

80. Boyle, S.; Rodesch, M.J.; Halvensleben, H.A.; Jeddeloh, J.A.; Bickmore, W.A. Fluorescence in situ hybridization with high-complexity repeat-free oligonucleotide probes generated by massively parallel synthesis. Chromosom. Res. 2011, 19, 901–909.

81. Hans de Jong, J.; Fransz, P.; Zabel, P. High resolution FISH in plants—Techniques and applications. Trends Plant Sci. 1999, 4, 258–263.

82. Gudla, P.R.; Nakayama, K.; Pegoraro, G.; Misteli, T. SpotLearn: Convolutional Neural Network for Detection of Fluorescence In Situ Hybridization (FISH) Signals in High-Throughput Imaging Approaches. Cold Spring Harb. Symp. Quant. Biol. 2017, 82, 57–70.

83. Mayer, R.; Brero, A.; von Hase, J.; Schroeder, T.; Cremer, T.; Dietzel, S. Common themes and cell type specific variations of higher order chromatin arrangements in the mouse. BMC Cell Biol. 2005, 6, 44.

84. Xie, S.Q.; Lavitas, L.-M.; Pombo, A. CryoFISH: Fluorescence In Situ Hybridization on Ultrathin Cryosections. In iFluorescence in situ Hybridization (FISH): Protocols and Applications; Bridger, J.M., Volpi, E.V., Eds.; Humana Press: Totowa, NJ, USA, 2010; pp. 219–230. ISBN 978-1-60761-789-1.

85. Branco, M.R.; Pombo, A. Intermingling of Chromosome Territories in Interphase Suggests Role in Translocations and Transcription-Dependent Associations. PLoS Biol. 2006, 4, e138.

86. Simonis, M.; Klous, P.; Splinter, E.; Moshkin, Y.; Willemsen, R.; de Wit, E.; van Steensel, B.; de Laat, W. Nuclear organization of active and inactive chromatin domains uncovered by chromosome conformation capture–on-chip (4C). Nat. Genet. 2006, 38, 1348–1354.

87. Beliveau, B.J.; Joyce, E.F.; Apostolopoulos, N.; Yilmaz, F.; Fonseka, C.Y.; McCole, R.B.; Chang, Y.; Li, J.B.; Senaratne, T.N.; Williams, B.R.; et al. Versatile design and synthesis platform for visualizing genomes with Oligopaint FISH probes. Proc. Natl. Acad. Sci. USA 2012, 109, 21301–21306.

88. Beliveau, B.J.; Apostolopoulos, N.; Wu, C. Visualizing Genomes with Oligopaint FISH Probes. Curr. Protoc. Mol. Biol. 2014, 105, 14.23.1–14.23.20.

89. Gnirke, A.; Melnikov, A.; Maguire, J.; Rogov, P.; LeProust, E.M.; Brockman, W.; Fennell, T.; Giannoukos, G.; Fisher, S.; Russ, C.; et al. Solution hybrid selection with ultra-long oligonucleotides for massively parallel targeted sequencing. Nat. Biotechnol. 2009, 27, 182–189.

90. Boettiger, A.N.; Bintu, B.; Moffitt, J.R.; Wang, S.; Beliveau, B.J.; Fudenberg, G.; Imakaev, M.; Mirny, L.A.; Wu, C.; Zhuang, X. Super-resolution imaging reveals distinct chromatin folding for different epigenetic states. Nature 2016, 529, 418–422.

91. Ni, Y.; Cao, B.; Ma, T.; Niu, G.; Huo, Y.; Huang, J.; Chen, D.; Liu, Y.; Yu, B.; Zhang, M.Q.; et al. Super-resolution imaging of a 2.5 kb non-repetitive DNA in situ in the nuclear genome using molecular beacon probes. eLife 2017, 6, e21660.

92. Di Stefano, M.; Di Giovanni, F.; Pozharskaia, V.; Gomar-Alba, M.; Baù, D.; Carey, L.B.; Marti-Renom, M.A.; Mendoza, M. Impact of Chromosome Fusions on 3D Genome Organization and Gene Expression in Budding Yeast. Genetics 2020, 214, 651–667.

93. Marchal, C.; Sima, J.; Gilbert, D.M. Control of DNA replication timing in the 3D genome. Nat. Rev. Mol. Cell Biol. 2019, 20, 721–737.

94. Smyk, M.; Szafranski, P.; Startek, M.; Gambin, A.; Stankiewicz, P. Chromosome conformation capture-on-chip analysis of long-range cis-interactions of the SOX9 promoter. Chromosom. Res. 2013, 21, 781–788.

95. Van de Werken, H.J.G.; Landan, G.; Holwerda, S.J.B.; Hoichman, M.; Klous, P.; Chachik, R.; Splinter, E.; Valdes-Quezada, C.; Öz, Y.; Bouwman, B.A.M.; et al. Robust 4C-seq data analysis to screen for regulatory DNA interactions. Nat. Methods 2012, 9, 969–972.

96. Loviglio, M.N.; Leleu, M.; Männik, K.; Passeggeri, M.; Giannuzzi, G.; van der Werf, I.; Waszak, S.M.; Zazhytska, M.; Roberts-Caldeira, I.; Gheldof, N.; et al. Chromosomal contacts connect loci associated with autism, BMI and head circumference phenotypes. Mol. Psychiatry 2017, 22, 836–849.

97. Dear, P.H.; Cook, P.R. Happy mapping: A proposal for linkage mapping the human genome. Nucleic Acids Res. 1989, 17, 6795–6807.

98. Stevens, T.J.; Lando, D.; Basu, S.; Atkinson, L.P.; Cao, Y.; Lee, S.F.; Leeb, M.; Wohlfahrt, K.J.; Boucher, W.; O'Shaughnessy-Kirwan, A.; et al. 3D structures of individual mammalian genomes studied by single-cell Hi-C. Nature 2017, 544, 59–64.

99. Gibcus, J.H.; Samejima, K.; Goloborodko, A.; Samejima, I.; Naumova, N.; Nuebler, J.; Kanemaki, M.T.; Xie, L.; Paulson, J.R.; Earnshaw, W.C.; et al. A pathway for mitotic chromosome formation. Science 2018, 359, eaao6135.
100. Bickmore, W.A. The Spatial Organization of the Human Genome. Annu. Rev. Genomics Hum. Genet. 2013, 14, 67–84.
101. Chen, B.; Gilbert, L.A.; Cimini, B.A.; Schnitzbauer, J.; Zhang, W.; Li, G.-W.; Park, J.; Blackburn, E.H.; Weissman, J.S.; Qi, L.S.; et al. Dynamic Imaging of Genomic Loci in Living Human Cells by an Optimized CRISPR/Cas System. Cell 2013, 155, 1479–1491.
102. Fudenberg, G.; Kelley, D.R.; Pollard, K.S. Predicting 3D genome folding from DNA sequence with Akita. Nat. Methods 2020, 17, 1111–1117.
103. Mullinger, A.M.; Johnson, R.T. Packing DNA into chromosomes. J. Cell Sci. 1980, 46, 61–86.
104. Luger, K.; Hansen, J.C. Nucleosome and chromatin fiber dynamics. Curr. Opin. Struct. Biol. 2005, 15, 188–196.
105. Belmont, A.S.; Sedat, J.W.; Agard, D.A. A three-dimensional approach to mitotic chromosome structure: Evidence for a complex hierarchical organization. J. Cell Biol. 1987, 105, 77–92.
106. Gibcus, J.H.; Dekker, J. The Hierarchy of the 3D Genome. Mol. Cell 2013, 49, 773–782.
107. Dorier, J.; Stasiak, A. Topological origins of chromosomal territories. Nucleic Acids Res. 2009, 37, 6316–6322.
108. Spilianakis, C.G.; Lalioti, M.D.; Town, T.; Lee, G.R.; Flavell, R.A. Interchromosomal associations between alternatively expressed loci. Nature 2005, 435, 637–645.
109. Lieberman-Aiden, E.; van Berkum, N.L.; Williams, L.; Imakaev, M.; Ragoczy, T.; Telling, A.; Amit, I.; Lajoie, B.R.; Sabo, P.J.; Dorschner, M.O.; et al. Comprehensive mapping of long-range interactions reveals folding principles of the human genome. Science 2009, 326, 289–293.
110. Dekker, J.; Misteli, T. Long-range chromatin interactions. Cold Spring Harb. Perspect. Biol. 2015, 7, a019356.
111. Mekhail, K.; Moazed, D. The nuclear envelope in genome organization, expression and stability. Nat. Rev. Mol. Cell Biol. 2010, 11, 317–328.
112. Van de Vosse, D.W.; Wan, Y.; Wozniak, R.W.; Aitchison, J.D. Role of the nuclear envelope in genome organization and gene expression. WIREs Syst. Biol. Med. 2011, 3, 147–166.
113. Kinney, N.A.; Onufriev, A.V.; Sharakhov, I. V Quantified effects of chromosome-nuclear envelope attachments on 3D organization of chromosomes. Nucleus 2015, 6, 212–224.
114. Lin, F.; Worman, H.J. Structural organization of the human gene encoding nuclear lamin A and nuclear lamin C. J. Biol. Chem. 1993, 268, 16321–16326.

115. Broers, J.L.V.; Kuijpers, H.J.H.; Östlund, C.; Worman, H.J.; Endert, J.; Ramaekers, F.C.S. Both lamin A and lamin C mutations cause lamina instability as well as loss of internal nuclear lamin organization. Exp. Cell Res. 2005, 304, 582–592.
116. Briand, N.; Collas, P. Lamina-associated domains: Peripheral matters and internal affairs. Genome Biol. 2020, 21, 85.
117. Van Steensel, B.; Belmont, A.S. Lamina-Associated Domains: Links with Chromosome Architecture, Heterochromatin, and Gene Repression. Cell 2017, 169, 780–791.
118. Maji, A.; Ahmed, J.A.; Roy, S.; Chakrabarti, B.; Mitra, M.K. A Lamin-Associated Chromatin Model for Chromosome Organization. Biophys. J. 2020, 118, 3041–3050.
119. Towbin, B.D.; Gonzalez-Sandoval, A.; Gasser, S.M. Mechanisms of heterochromatin subnuclear localization. Trends Biochem. Sci. 2013, 38, 356–363.
120. Mattout, A.; Cabianca, D.S.; Gasser, S.M. Chromatin states and nuclear organization in development—A view from the nuclear lamina. Genome Biol. 2015, 16, 174.
121. Imai, S.; Nishibayashi, S.; Takao, K.; Tomifuji, M.; Fujino, T.; Hasegawa, M.; Takano, T. Dissociation of Oct-1 from the Nuclear Peripheral Structure Induces the Cellular Aging-associated Collagenase Gene Expression. Mol. Biol. Cell 1997, 8, 2407–2419.
122. Lanctôt, C.; Cheutin, T.; Cremer, M.; Cavalli, G.; Cremer, T. Dynamic genome architecture in the nuclear space: Regulation of gene expression in three dimensions. Nat. Rev. Genet. 2007, 8, 104–115.
123. Fraser, P.; Bickmore, W. Nuclear organization of the genome and the potential for gene regulation. Nature 2007, 447, 413–417.
124. Finlan, L.E.; Sproul, D.; Thomson, I.; Boyle, S.; Kerr, E.; Perry, P.; Ylstra, B.; Chubb, J.R.; Bickmore, W.A. Recruitment to the Nuclear Periphery Can Alter Expression of Genes in Human Cells. PLoS Genet. 2008, 4, e1000039.
125. Lemaître, C.; Bickmore, W.A. Chromatin at the nuclear periphery and the regulation of genome functions. Histochem. Cell Biol. 2015, 144, 111–122.
126. Gruenbaum, Y.; Margalit, A.; Goldman, R.D.; Shumaker, D.K.; Wilson, K.L. The nuclear lamina comes of age. Nat. Rev. Mol. Cell Biol. 2005, 6, 21–31.
127. Karoutas, A.; Akhtar, A. Functional mechanisms and abnormalities of the nuclear lamina. Nat. Cell Biol. 2021, 23, 116–126.
128. Bridger, J.M.; Foeger, N.; Kill, I.R.; Herrmann, H. The nuclear lamina. FEBS J. 2007, 274, 1354–1361.

129. Pepenella, S.; Hayes, J. Global histone acetylation induces functional genomic reorganization at mammalian nuclear pore complexes: Commentary. Chemtracts 2007, 20, 406–409.

130. Ptak, C.; Aitchison, J.D.; Wozniak, R.W. The multifunctional nuclear pore complex: A platform for controlling gene expression. Curr. Opin. Cell Biol. 2014, 28, 46–53.

131. Németh, A.; Längst, G. Genome organization in and around the nucleolus. Trends Genet. 2011, 27, 149–156.

132. Pontvianne, F.; Carpentier, M.-C.; Durut, N.; Pavlištová, V.; Jaške, K.; Schořová, Š.; Parrinello, H.; Rohmer, M.; Pikaard, C.S.; Fojtová, M.; et al. Identification of Nucleolus-Associated Chromatin Domains Reveals a Role for the Nucleolus in 3D Organization of the A. thaliana Genome. Cell Rep. 2016, 16, 1574–1587.

133. Németh, A.; Conesa, A.; Santoyo-Lopez, J.; Medina, I.; Montaner, D.; Péterfia, B.; Solovei, I.; Cremer, T.; Dopazo, J.; Längst, G. Initial Genomics of the Human Nucleolus. PLoS Genet. 2010, 6, e1000889.

134. Therizols, P.; Duong, T.; Dujon, B.; Zimmer, C.; Fabre, E. Chromosome arm length and nuclear constraints determine the dynamic relationship of yeast subtelomeres. Proc. Natl. Acad. Sci. USA 2010, 107, 2025–2030.

135. Duan, Z.; Andronescu, M.; Schutz, K.; McIlwain, S.; Kim, Y.J.; Lee, C.; Shendure, J.; Fields, S.; Blau, C.A.; Noble, W.S. A three-dimensional model of the yeast genome. Nature 2010, 465, 363–367.

136. Meaburn, K.J.; Misteli, T. Chromosome territories. Nature 2007, 445, 379–381.

137. Wang, Y.; Botvinick, E.L.; Zhao, Y.; Berns, M.W.; Usami, S.; Tsien, R.Y.; Chien, S. Visualizing the mechanical activation of Src. Nature 2005, 434, 1040–1045.

138. Le, H.Q.; Ghatak, S.; Yeung, C.-Y.C.; Tellkamp, F.; Günschmann, C.; Dieterich, C.; Yeroslaviz, A.; Habermann, B.; Pombo, A.; Niessen, C.M.; et al. Mechanical regulation of transcription controls Polycomb-mediated gene silencing during lineage commitment. Nat. Cell Biol. 2016, 18, 864–875.

139. Nakazawa, N.; Sathe, A.R.; Shivashankar, G.V.; Sheetz, M.P. Matrix mechanics controls FHL2 movement to the nucleus to activate p21 expression. Proc. Natl. Acad. Sci. USA 2016, 113, E6813–E6822.

140. Jain, N.; Iyer, K.V.; Kumar, A.; Shivashankar, G. V Cell geometric constraints induce modular gene-expression patterns via redistribution of HDAC3 regulated by actomyosin contractility. Proc. Natl. Acad. Sci. USA 2013, 110, 11349–11354.

141. Chen, C.S.; Mrksich, M.; Huang, S.; Whitesides, G.M.; Ingber, D.E. Geometric Control of Cell Life and Death. Science 1997, 276, 1425–1428.

142. Kilian, K.A.; Bugarija, B.; Lahn, B.T.; Mrksich, M. Geometric cues for directing the differentiation of mesenchymal stem cells. Proc. Natl. Acad. Sci. USA 2010, 107, 4872–4877.

143. Thomas, C.H.; Collier, J.H.; Sfeir, C.S.; Healy, K.E. Engineering gene expression and protein synthesis by modulation of nuclear shape. Proc. Natl. Acad. Sci. USA 2002, 99, 1972–1977.

144. Suter, D.M.; Molina, N.; Gatfield, D.; Schneider, K.; Schibler, U.; Naef, F. Mammalian Genes Are Transcribed with Widely Different Bursting Kinetics. Science 2011, 332, 472–474.

145. Bartman, C.R.; Hamagami, N.; Keller, C.A.; Giardine, B.; Hardison, R.C.; Blobel, G.A.; Raj, A. Transcriptional Burst Initiation and Polymerase Pause Release Are Key Control Points of Transcriptional Regulation. Mol. Cell 2019, 73, 519–532.e4.

146. Chen, H.; Levo, M.; Barinov, L.; Fujioka, M.; Jaynes, J.B.; Gregor, T. Dynamic interplay between enhancer–promoter topology and gene activity. Nat. Genet. 2018, 50, 1296–1303.

147. Cho, W.-K.; Jayanth, N.; English, B.P.; Inoue, T.; Andrews, J.O.; Conway, W.; Grimm, J.B.; Spille, J.-H.; Lavis, L.D.; Lionnet, T.; et al. RNA Polymerase II cluster dynamics predict mRNA output in living cells. eLife 2016, 5, e13617.

148. Fanucchi, S.; Shibayama, Y.; Burd, S.; Weinberg, M.S.; Mhlanga, M.M. Chromosomal Contact Permits Transcription between Coregulated Genes. Cell 2013, 155, 606–620.

149. Noordermeer, D.; Leleu, M.; Schorderet, P.; Joye, E.; Chabaud, F.; Duboule, D. Temporal dynamics and developmental memory of 3D chromatin architecture at Hox gene loci. eLife 2014, 3, e02557.

150. Letsou, W.; Cai, L. Noncommutative Biology: Sequential Regulation of Complex Networks. PLoS Comput. Biol. 2016, 12, e1005089.

151. Schreiber, K.H.; Kennedy, B.K. When lamins go bad: Nuclear structure and disease. Cell 2013, 152, 1365–1375.

152. Hatch, E.; Hetzer, M. Breaching the nuclear envelope in development and disease. J. Cell Biol. 2014, 205, 133–141.

153. Finch, J.T.; Klug, A. Solenoidal model for superstructure in chromatin. Proc. Natl. Acad. Sci. USA 1976, 73, 1897–1901.

154. Ou, H.D.; Phan, S.; Deerinck, T.J.; Thor, A.; Ellisman, M.H.; O'Shea, C.C. ChromEMT: Visualizing 3D chromatin structure and compaction in interphase and mitotic cells. Science 2017, 357, eaag0025.

155. Banigan, E.J.; Mirny, L.A. Loop extrusion: Theory meets single-molecule experiments. Curr. Opin. Cell Biol. 2020, 64, 124–138.

156. Terakawa, T.; Bisht, S.; Eeftens, J.M.; Dekker, C.; Haering, C.H.; Greene, E.C. The condensin complex is a mechanochemical motor that translocates along DNA. Science 2017, 358, 672–676.

157. Kelman, Z.; O'Donnell, M. DNA polymerase III holoenzyme: Structure and function of a chromosomal replicating machine. Annu. Rev. Biochem. 1995, 64, 171–200.

158. Wang, M.D.; Schnitzer, M.J.; Yin, H.; Landick, R.; Gelles, J.; Block, S.M. Force and Velocity Measured for Single Molecules of RNA Polymerase. Science 1998, 282, 902–907.

159. Bintu, B.; Mateo, L.J.; Su, J.-H.; Sinnott-Armstrong, N.A.; Parker, M.; Kinrot, S.; Yamaya, K.; Boettiger, A.N.; Zhuang, X. Super-resolution chromatin tracing reveals domains and cooperative interactions in single cells. Science 2018, 362, eaau1783.

160. Szabo, Q.; Jost, D.; Chang, J.-M.; Cattoni, D.I.; Papadopoulos, G.L.; Bonev, B.; Sexton, T.; Gurgo, J.; Jacquier, C.; Nollmann, M.; et al. TADs are 3D structural units of higher-order chromosome organization in Drosophila. Sci. Adv. 2018, 4, eaar8082.

161. Huang, K.; Li, Y.; Shim, A.R.; Nap, R.J.; Agrawal, V.; Virk, R.K.A.; Eshein, A.; Almassalha, L.M.; Backman, V.; Szleifer, I. Physical and data structure of 3D genome. Sci. Adv. 2020, 6, eaay4055.

162. Rabin, A.; Neer, A. Crumpled Globule Model of the Three-Dimensional Structure of DNA. EPL (Europhys. Lett.) 2006, 23, 373.

163. Mirny, L.A. The fractal globule as a model of chromatin architecture in the cell. Chromosome Res. 2011, 19, 37–51.

164. Bianco, S.; Chiariello, A.M.; Conte, M.; Esposito, A.; Fiorillo, L.; Musella, F.; Nicodemi, M. Computational approaches from polymer physics to investigate chromatin folding. Curr. Opin. Cell Biol. 2020, 64, 10–17.

165. Dekker, J.; Belmont, A.S.; Guttman, M.; Leshyk, V.O.; Lis, J.T.; Lomvardas, S.; Mirny, L.A.; O'Shea, C.C.; Park, P.J.; Ren, B.; et al. The 4D nucleome project. Nature 2017, 549, 219–226.

166. Nicodemi, M.; Prisco, A. Thermodynamic Pathways to Genome Spatial Organization in the Cell Nucleus. Biophys. J. 2009, 96, 2168–2177.

167. Jost, D.; Carrivain, P.; Cavalli, G.; Vaillant, C. Modeling epigenome folding: Formation and dynamics of topologically associated chromatin domains. Nucleic Acids Res. 2014, 42, 9553–9561.

168. Chiariello, A.M.; Annunziatella, C.; Bianco, S.; Esposito, A.; Nicodemi, M. Polymer physics of chromosome large-scale 3D organisation. Sci. Rep. 2016, 6, 29775.

169. Bianco, S.; Lupiáñez, D.G.; Chiariello, A.M.; Annunziatella, C.; Kraft, K.; Schöpflin, R.; Wittler, L.; Andrey, G.; Vingron, M.; Pombo, A.; et al. Polymer physics predicts the effects of structural variants on chromatin architecture. Nat. Genet. 2018, 50, 662–667.

170. Brackley, C.A.; Johnson, J.; Kelly, S.; Cook, P.R.; Marenduzzo, D. Simulated binding of transcription factors to active and inactive regions folds human chromosomes into loops, rosettes and topological domains. Nucleic Acids Res. 2016, 44, 3503–3512.

171. Erdel, F.; Rippe, K. Formation of Chromatin Subcompartments by Phase Separation. Biophys. J. 2018, 114, 2262–2270.

172. Weintraub, A.S.; Li, C.H.; Zamudio, A.V.; Sigova, A.A.; Hannett, N.M.; Day, D.S.; Abraham, B.J.; Cohen, M.A.; Nabet, B.; Buckley, D.L.; et al. YY1 Is a Structural Regulator of Enhancer-Promoter Loops. Cell 2017, 171, 1573–1588.e28.

173. Zhou, X.; Maricque, B.; Xie, M.; Li, D.; Sundaram, V.; Martin, E.A.; Koebbe, B.C.; Nielsen, C.; Hirst, M.; Farnham, P.; et al. The Human Epigenome Browser at Washington University. Nat. Methods 2011, 8, 989–990.

174. Zhou, X.; Lowdon, R.F.; Li, D.; Lawson, H.A.; Madden, P.A.F.; Costello, J.F.; Wang, T. Exploring long-range genome interactions using the WashU Epigenome Browser. Nat. Methods 2013, 10, 375–376.

175. Durand, N.C.; Robinson, J.T.; Shamim, M.S.; Machol, I.; Mesirov, J.P.; Lander, E.S.; Aiden, E.L. Juicebox Provides a Visualization System for Hi-C Contact Maps with Unlimited Zoom. Cell Syst. 2016, 3, 99–101.

176. Kerpedjiev, P.; Abdennur, N.; Lekschas, F.; McCallum, C.; Dinkla, K.; Strobelt, H.; Luber, J.M.; Ouellette, S.B.; Azhir, A.; Kumar, N.; et al. HiGlass: Web-based visual exploration and analysis of genome interaction maps. Genome Biol. 2018, 19, 125.

177. Tang, B.; Li, F.; Li, J.; Zhao, W.; Zhang, Z. Delta: A new web-based 3D genome visualization and analysis platform. Bioinformatics 2018, 34, 1409–1410.

178. Wang, Y.; Song, F.; Zhang, B.; Zhang, L.; Xu, J.; Kuang, D.; Li, D.; Choudhary, M.N.K.; Li, Y.; Hu, M.; et al. The 3D Genome Browser: A web-based browser for visualizing 3D genome organization and long-range chromatin interactions. Genome Biol. 2018, 19, 151.